

# Biocatalytic oxidation by chloroperoxidase from *Caldariomyces fumago* in polymersome nanoreactors†‡

H. M. de Hoog,<sup>a</sup> M. Nallani,<sup>a,b</sup> J. J. L. M. Cornelissen,<sup>\*a,c</sup> A. E. Rowan,<sup>a</sup> R. J. M. Nolte<sup>a</sup> and I. W. C. E. Arends<sup>\*d</sup>

Received 10th June 2009, Accepted 29th July 2009

First published as an Advance Article on the web 3rd September 2009

DOI: 10.1039/b911370c

The encapsulation of chloroperoxidase from *Caldariomyces fumago* (CPO) in block copolymer polymersomes is reported. Fluorescence and electron microscopy show that when the encapsulating conditions favour self-assembly of the block copolymer, the enzyme is incorporated with concentrations that are 50 times higher than the enzyme concentration before encapsulation. The oxidation of two substrates by the encapsulated enzyme was studied: i) pyrogallol, a common substrate used to assay CPO enzymatic activity and ii) thioanisole, of which the product, (*R*)-methyl phenyl sulfoxide, is an important pharmaceutical intermediate. The CPO-loaded polymersomes showed distinct reactivity towards these substrates. While the oxidation of pyrogallol was limited by diffusion of the substrate into the polymersome, the rate-limiting step for the oxidation of thioanisole was the turnover by the enzyme.

## Introduction

Biohybrid compounds that are able to form sub-micrometer (*i.e.* nano-) stable capsules in an aqueous environment by self-assembly are of interest to the biomedical and physical fields from both a fundamental and applied perspective.<sup>1,2</sup> When loaded with therapeutic proteins or enzymes, and made responsive to external stimuli, these capsules may be used in diagnostics or targeted drug delivery. For diagnostics, the ideal system combines permeability to analytes with shielding of its contents to the environment.<sup>3</sup> Ideally, drugs or gene vectors loaded into nano-capsules are protected from the biological surroundings, but should be readily released once ingested by the target cell.<sup>4</sup> Alternatively, one could envision self-assembled nano-capsules as mild immobilization agents for enzymes to perform environmentally benign biotransformations.<sup>5,6</sup> Immobilization of biocatalysts is widely applied for the stabilization of the generally labile enzyme and facilitates removal of the catalyst from the reaction mixture. Often, immobilization is accompanied by activity loss as a result of either diffusion limitation or the fact that the enzyme has now become a heterogeneous instead of a homogeneous catalyst. Encapsulation of enzymes into the nano-sized volumes of porous polymer capsules diminishes the diffusion limitation while retaining the homogeneous nature of the system.

In recent decades we have seen the emergence of vesicular systems as scaffolds for the harboring of enzymes, of which the most thoroughly studied systems are liposomes. Although progress in the entrapping of enzymes has been made, liposomes generally lack stability and disintegrate over time.<sup>7,8</sup> In addition, the permeability of the vesicle bilayers for externally added substrate molecules is usually low.<sup>8</sup> These shortcomings have been addressed by cross-linking the membrane and/or by the incorporation of membrane channels.<sup>9</sup> Recently, bottom-up engineered nano-sized capsule systems have emerged based on (amphiphilic) polymers, allowing the tuning of the properties of the corresponding particles.<sup>10</sup> This has led to a diversity of functional nano-reactors containing enzymes.<sup>5,11-14</sup> An interesting approach involves layer-by-layer (LbL) assembly, by which oppositely charged polyelectrolytes are adsorbed on a sacrificial template.<sup>15,16</sup> This technique allows the incorporation of enzymes while an attractive characteristic is the capability to modulate permeability of the thus-prepared capsule.<sup>17</sup> In addition, spatial confinement of different enzymes in the LbL-constructs has been shown recently.<sup>18</sup> Magnetic nanoparticles constitute another emerging platform of enzyme immobilization, of which the main advantage is the ease by which the catalyst can be removed from the reaction mixture.<sup>19</sup>

A promising approach for the synthesis of nano-sized capsules involves the direct self-assembly of amphiphilic block copolymers into polymersomes.<sup>20,21</sup> These structures are reminiscent of liposomes but exhibit enhanced stability, and the possibility to encapsulate enzymes has been reported.<sup>22</sup> As stability often comes with reduced permeability, polymersomes have been equipped with trans-membrane channels even though their membrane dimensions exceed that of the natural cell membrane.<sup>23,24</sup> Furthermore, polymersomes have been exploited as a platform to covalently attach enzymes.<sup>25-27</sup> Interesting functional systems have been created based on the triblock copolymer PMOXA-PDMS-PMOXA, ranging from pH-switchable nano-reactors to nano-compartments for the selective recovery of DNA.<sup>23,28</sup> Unique in this aspect are polymersomes assembled from polystyrene-*b*-poly(L-isocyanalanine-(2-thiophene-3-yl-ethyl)amide) (PS-PIAT), which are permeable

<sup>a</sup>Institute for Molecules and Materials, Radboud University Nijmegen, Heyendaalseweg 135, 6525 AJ, Nijmegen, The Netherlands

<sup>b</sup>Institute of Materials Research & Engineering (IMRE), Research Link 3, Singapore 117602

<sup>c</sup>Laboratory for Biomolecular Nanotechnology, MESA+ Institute, University of Twente, P.O. Box 217, 7500 AE, Enschede, the Netherlands. E-mail: J.J.L.M. Cornelissen@tmw.utwente.nl; Fax: +3153 489 4645; Tel: +31 53 489 4380

<sup>d</sup>Dept. of Biotechnology, Delft University of Technology, Julianalaan 136, 2628 DL, Delft, The Netherlands. E-mail: I.W.C.E.Arends@tudelft.nl

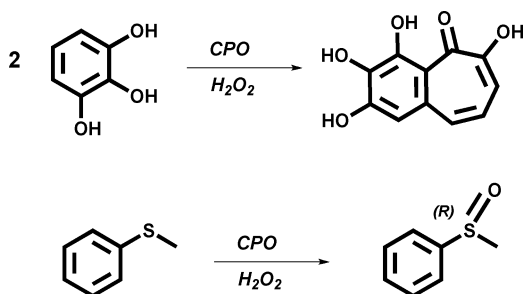
† Electronic supplementary information (ESI) available: Experimental procedures and additional characterization. See DOI: 10.1039/b911370c

‡ This paper is part of an *Organic & Biomolecular Chemistry* web theme issue on biocatalysis.

to low-molecular weight organic molecules but at the same time are able to retain enzymes.<sup>29,30</sup> Furthermore, the positional assembly of enzymes in either the membrane or the aqueous inner compartment of PS-PIAT polymersomes has recently been described.<sup>31</sup>

Enzymes are environmentally benign catalysts and well suited for the synthesis of enantiopure synthons, which is of importance to the fine-chemical and pharmaceutical industries.<sup>32</sup> This fact has inspired us to encapsulate industrially relevant enzymes inside PS-PIAT polymersomes and study their activity. Conversion of industrially interesting substrates in polymersomes has not been demonstrated so far. Moreover, studies on nano-scale enzyme reactors in aqueous environment generally are limited to substrates selected on their desirable spectroscopic properties.<sup>3,6,11-14,17,33,34</sup> Often, these substrates include fast-reacting and activated compounds like *p*-nitrophenyl adducts, the structure of which relies on the type of enzyme. Organic synthons do not exhibit these favourable properties and generally react at different rates, depending on solubility and affinity and, probably as a consequence of this, have been studied in much less detail.

As an example of a potential biocatalyst useful to organic synthesis, we decided to incorporate chloroperoxidase from *Caldariomyces fumago* (CPO; EC 1.1.11.1) into the polymersomes. CPO fills the niche between the cofactor-dependant cytochrome P450 oxygenases and the hemeperoxidases, and is unique in its ability to catalyze the enantioselective epoxidation of a variety of alkenes.<sup>35</sup> Its industrial application is, however, still hindered by the rapid deactivation of the enzyme in the presence of oxidant. At this moment the mechanism of deactivation is not well understood but seems to result from degradation of the heme-group of the enzyme or the oxidation of the axial cysteine ligand.<sup>36</sup> Encapsulation of CPO into polymersomes might have a stabilizing effect on the limited operational stability of the enzyme. In this paper, we report on a first step in this direction, *i.e.*, by the functional encapsulation of CPO into PS-PIAT polymersomes and the study of the oxidation of two different substrates (Scheme 1). We found that the oxidation of pyrogallol to purpurogallin, a reaction commonly used to assay peroxidase activity, shows a different kinetic behaviour than the oxidation of thioanisole to (*R*)-phenyl methyl sulfoxide – a chiral pharmaceutical intermediate.



**Scheme 1** Chloroperoxidase-catalyzed reactions studied in this work.

## Results and discussion

### Encapsulation of chloroperoxidase

In general, the incorporation of enzymes into PS-PIAT polymersomes is achieved by addition of 1 volume of a PS-PIAT

solution in THF (1 mg ml<sup>-1</sup>) to 5 volumes of an aqueous solution containing enzymes (0.2–2 mg ml<sup>-1</sup>).<sup>31,37</sup> During formation of the polymersomes by self-assembly, statistically a fraction of the enzymes is incorporated into the polymersomes. The solution is left to equilibrate for 24 hours and the turbid solution is filtered, to remove the non-encapsulated enzyme. Both the enzymatic activity of the flow-throughs and the activity of the supernatant containing the polymersomes is measured. Ideally, after sufficient washings the activity of the flow-throughs reaches zero while the activity of the supernatant is retained, demonstrating the incorporation of the enzyme into the polymersomes.

For incorporation of CPO inside the polymersomes the procedure was adjusted. First, the final volume percentage of THF was lowered, because at the initial volume percentage (20% v/v) the enzyme was irreversibly deactivated (Fig. S1†), as was observed by determining its chlorinating activity in the presence of increasing amounts of THF.<sup>38</sup> It was found that at a concentration of 10% THF the enzyme showed similar activity as the enzyme in aqueous buffer. In order to have a concentration of PS-PIAT similar to the previously used conditions for the successful encapsulation of enzymes, the initial concentration of PS-PIAT in THF was doubled.

Although the enzyme retained its activity in aqueous THF, encapsulation in PS-PIAT polymersomes was not successful under the conditions (pH = 3, 0.1 M phosphate/citric acid buffer) used in a halogenation assay. After several washings with buffer no chlorination activity was left in the flow-throughs or in the supernatant, indicating that all active protein was washed out. Upon examination of the unfiltered polymersomes by TEM, spherical aggregates were still visible, ranging in diameter from ~500 nm (the size of the regular enzyme-containing polymersomes) to aggregates of more than 10 μm (Fig. S2†). Clearly the combination of enzyme and buffer has a noticeable effect on the aggregation properties of the PS-PIAT and apparently affects the encapsulation as well. This is also the case for previously encapsulated enzymes like CALB, HRP and GOx, of which the resulting polymersomes showed varying sizes and different membrane characteristics.<sup>31,37</sup> In addition, dispersions of empty polymersomes precipitated after a few days, whereas co-aggregates of PS-PIAT and proteins stayed intact for months.<sup>30</sup>

As encapsulation of PS-PIAT at the standard operating conditions of CPO was not trivial, CPO was incorporated under the self-assembly conditions reported for PS-PIAT (milli-Q; pH ~ 6). It was observed that under these unbuffered conditions the enzyme did not behave differently than at pH = 5 in 50 mM acetate buffer (Fig. S3†). At pH 5 or above the halogenating activity of CPO is lost but the enzyme is still active in the oxidation of various substrates, which is our reaction of interest.<sup>35,39,40</sup> The CPO-polymersome (CP) activity was measured as the rate of oxidation of pyrogallol to purpurogallin (Scheme 1).<sup>41</sup> The oxidation activity apparently was not affected by the presence of THF.

After preparation of the polymersomes and filtering the dispersion, it was found that the oxidation activity was retained in the supernatant, indicating encapsulation of the enzyme inside the polymersomes. Investigation of the aggregates by TEM revealed the presence of spherical objects, which, in contrast to the typical membrane-structure observed for empty polymersomes, showed a uniform density. However, upon closer inspection the membrane was clearly visible (Fig. S4†). Interestingly, functional

encapsulation only occurred at starting concentrations of CPO of  $3 \mu\text{M}$  ( $0.1 \text{ mg ml}^{-1}$ ) or higher. Based on the activity of the resulting CPs in the oxidation of pyrogallol, the starting concentration of CPO (*i.e.* the concentration of CPO before filtering) did not seem to have an effect on the eventual activity of the aggregates (Fig. 1). Varying the starting concentration of CPO between 7, 23 and  $36 \mu\text{M}$  ( $0.3$ ,  $0.9$  and  $1.5 \text{ mg ml}^{-1}$ ) resulted in an activity between  $0.4 \text{ abs min}^{-1}$  and  $0.6 \text{ abs min}^{-1}$ , and was lowest for the CPs with a starting concentration of  $23 \mu\text{M}$ . In contrast, activity measurements with the free enzyme in a similar activity range showed a linear relation between activity and enzyme concentration (Fig. 1 inset). From a comparison with the data-points in the graph in the inset, the apparent amount of enzyme in the polymersomes can be calculated. For the CPs prepared from a  $23 \mu\text{M}$  CPO solution, an activity was found of  $0.4 \text{ abs min}^{-1}$ . This corresponds to a concentration of  $0.1 \mu\text{M}$ , indicating an encapsulation efficiency of  $0.5\%$ . Although this is a small number, a low value may be expected when the estimated volume fraction of the polymersomes is taken into account ( $0.1\%$ ), and it is assumed that encapsulation is based solely on statistics.<sup>31</sup> On the other hand, the activity of the CPs was found to be considerably lower than observed previously.<sup>31</sup>

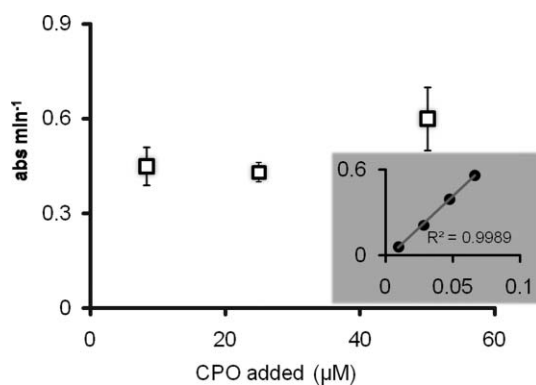


**Fig. 1** Enzymatic activity measured at  $\lambda = 420 \text{ nm}$  by the pyrogallol assay ( $\text{abs min}^{-1}$ ) of CPs obtained by filtration of CPO/PS-PIAT dispersions with increasing concentrations of enzyme ( $\mu\text{M}$ ). The inset shows the dependence of the activity on the concentration of the free enzyme ( $\mu\text{M}$ ) in the same activity range ( $\text{abs min}^{-1}$ ).

The observed results prompted us to investigate in more detail the concentration and the location of CPO in the polymersomes. Since the concentration of CPO can be determined from the absorbance of the heme group at  $\lambda = 400 \text{ nm}$ , the concentration of CPO inside the polymersomes was determined by UV-Vis measurements on the aggregate solutions.<sup>42</sup> The data showed large absorption/scattering from the polymersomes, but also the distinct absorption of the enzyme was visible (Fig. 2; left graph). To estimate the concentrations of the CPO inside the polymersomes, the absorbance of the empty polymersomes was subtracted from the absorption of the CPs. These calculations showed that unlike the outcome of the pyrogallol activity measurements, the concentration of enzyme inside the polymersomes increased linearly from  $0.05$  to  $2 \mu\text{M}$  with increasing starting concentration of enzyme (Table 1). Interestingly, the measured concentration of the enzyme inside the polymersomes appeared to be considerably higher than the concentration that was determined from the activity tests.

**Table 1** Concentration of CPO, as determined by UV-vis, in the initial polymersome preparation (before filtration) and in the filtered dispersion. Also shown is the estimated local concentration of the enzyme in the volume of the polymersomes

	Initial CPO concentration ( $\mu\text{M}$ ) <sup>a</sup>		
	9 ( $\pm 4$ )	23	36
Mean concentration in filtered solution ( $\mu\text{M}$ ) <sup>a</sup>	0.05 ( $\pm 0.04$ )	0.9 ( $\pm 0.4$ )	2 ( $\pm 0.4$ )
Encapsulation (%)	0.6	4.0	5.9
Local concentration in CPs ( $\text{mM}$ ) <sup>b</sup>	0.05	0.8	2.0

<sup>a</sup> Mean of 3 measurements. <sup>b</sup> Based on the assumption that the volume fraction of the polymersomes is  $0.0011$  and encapsulation occurs statistically.<sup>31</sup>

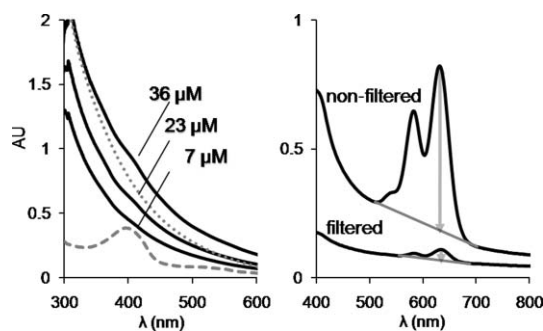


**Fig. 2** (Left) UV-Vis spectra of CPs containing different loadings of CPO (solid line). The absorption spectrum of free CPO exhibiting the characteristic absorption of the heme at  $\lambda = 420 \text{ nm}$  (dashed line) is shown, as well as the absorption spectrum of empty polymersomes (dotted line). (Right) Absorption spectra of a dispersion of PS-PIAT and CPO labelled with Alexa-633 dye, before and after filtering off the non-encapsulated enzyme. The initial concentration of CPO was  $23 \mu\text{M}$ . The straight lines underneath the absorption peaks were taken as the base-line for the calculation of the ratio between the peaks.

To probe the location of the enzyme inside the polymersomes, the enzyme was labeled with the fluorescent dye Alexa-633 and encapsulated, after which the encapsulated system was studied with confocal fluorescence microscopy (CFM, Fig. 3). Polymersomes containing the labeled enzyme were prepared following

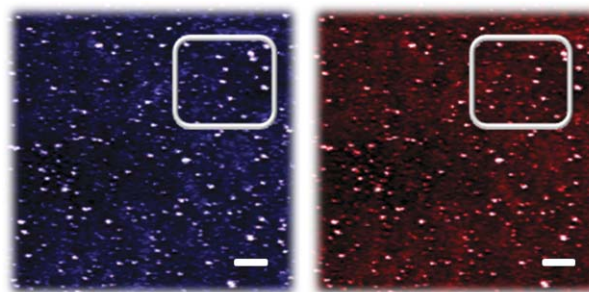


**Fig. 3** (Left; blue) Confocal scanning fluorescence microscope image at  $\lambda_{\text{em}} = 505 \text{ nm}$  of polymersomes loaded with Alexa-633 labeled CPO (initial concentration  $23 \mu\text{M}$ ) showing fluorescence of the PS-PIAT itself. (Right; red) Fluorescence image at  $\lambda_{\text{em}} = 650 \text{ nm}$  of polymersomes loaded with labeled CPO showing the emission from the labeled CPO. The polymersome distribution on the substrate is the same at both wavelengths, as is emphasized by the white squares. For fluorescence images of non-labeled CPO encapsulated in the polymersomes at both emission wavelengths; see Fig. S5†.

exactly the same procedure as was used for the non-labeled enzyme (enzyme concentration before filtration = 23  $\mu\text{M}$ ). The fluorescence emission from the CPs containing the labeled CPO and the non-labeled protein was then studied both at  $\lambda_{\text{em}} = 505 \text{ nm}$  ( $\lambda_{\text{ex}} = 488 \text{ nm}$ ) and  $\lambda_{\text{em}} = 650 \text{ nm}$  ( $\lambda_{\text{ex}} = 633$ ). At  $\lambda_{\text{em}} = 505 \text{ nm}$  for both systems emission was observed, originating from the PS-PIAT polymer itself (as emission from the dye is absent below  $\lambda = 600 \text{ nm}$ ). When  $\lambda_{\text{ex}} = 633 \text{ nm}$  a different pattern was found, that is, fluorescence emission was only observed for CPs with labeled CPO. No signal was observed for the CPs containing non-labeled enzyme. Furthermore when overlaying the fluorescence images at  $\lambda_{\text{em}} = 505 \text{ nm}$  and  $\lambda_{\text{em}} = 650 \text{ nm}$  of CPs containing labeled CPO, the same distribution pattern was observed (Fig. 3), confirming that CPO was located inside the polymersomes.

The dye labeling also provided a means of determining the concentration of CPO inside the polymersomes more accurately (Fig. 2; right graph). The labeled CPO shows an intense absorption at  $\lambda = 633 \text{ nm}$ , and this signal is virtually undisturbed by the adsorption from the polymersomes compared to the signal of the heme at  $\lambda = 400 \text{ nm}$ . The ratio in absorption between the filtered CPs and the CPs before filtration gives the percentage of encapsulation, which for a labeled CPO solution containing an initial concentration of 23  $\mu\text{M}$  enzyme gives an encapsulation efficiency of 4%. Moreover, dye labeling experiments with initial CPO concentrations of 9, 18, 27 to 36  $\mu\text{M}$  showed a concurrent, linear increase in CPO concentration after filtration, indicating that the encapsulation efficiency was constant over the concentrations studied. These results correlated with the calculations based on the UV-Vis measurements on the unlabeled protein encapsulated in the polymersomes. The CPs prepared from 7  $\mu\text{M}$  CPO solutions give a slightly lower value, which might be the result of disturbance of the heme-signal by the absorption/scattering of the polymersomes. For the CPs prepared from 36  $\mu\text{M}$  CPO solutions, the enzyme concentration appears to be 50 times what it would be if encapsulation is considered to be a purely statistical process. Assuming that the volume fraction of the polymersomes is 0.0011,<sup>31</sup> this would lead to a concentration of  $\sim 0.04 \mu\text{M}$ . In the present case, the local concentration of the enzyme inside the polymersomes is estimated to be 2.0 mM (Table 1). This is a considerable concentration, and may explain partly why for CALB, HRP and GOx it was found that the encapsulated enzyme was 100-fold more active than the free enzyme.<sup>31</sup>

The reduced activity of the CPs in the oxidation of pyrogallol, and the non-linear variation of the activity of the CPs in the oxidation of pyrogallol with increasing enzyme-loading, points to diffusion limitation which is imposed by locating the enzyme inside the polymersomes. Most likely this effect results from the substrate having to cross the physical barrier of the block copolymer membrane in order to reach the active site of the enzyme (see later).

### Sulfoxidation inside CPs

Following the successful encapsulation of CPO in the polymersomes and the study of the oxidation of pyrogallol, we decided to also study the conversion of a relevant model organic synthon. For these investigations the sulfoxidation of thioanisole (methyl phenyl sulfide) to (*R*)-methyl phenyl sulfoxide was chosen (Scheme 1). Chiral sulfoxides have been used in asymmetric synthesis as

valuable chiral auxiliaries, and the sulfoxyl moiety is frequently found in bioactive natural products and synthetic drugs.<sup>43</sup> The enzymatic oxidation of this compound by CPO has been studied in detail in the field of biocatalysis.<sup>44–47</sup> Depending on the conditions used the reaction affords the corresponding (*R*)-sulfoxide in high ee (99%) and high yields. When the enzyme concentration is kept sufficiently high, oxidation occurs very rapidly, thereby avoiding the non-enzymatic oxidation of the substrate.

It turned out that sulfoxidation also proceeded readily inside the CPs, showing that the structure of the polymersomes allowed substrate and oxidant to reach the active site of the enzyme and did not hamper the introduction of the oxygen into the substrate. Furthermore, based on gas chromatography (GC), the polymersome-anchored enzyme allowed the formation of the desired sulfoxide in the same high enantioselectivity as observed for the free enzyme. When the oxidation of thioanisole by the CPs was followed over time, a subtle effect of the polymersome structure on the kinetics was observed (Fig. 4). Although the initial rates of the CPs and free CPO were of the same order of magnitude, the free CPO at a concentration of 60 nM (comparable apparent activity as the encapsulated enzyme) already showed 100% conversion of substrate after 2 minutes, whereas for the CPs thioanisole conversion was only 39–65%. When the concentration of free CPO was increased to 1  $\mu\text{M}$  (concentration determined by UV for the enzyme concentration inside the polymersomes), full conversion was already observed after 40 seconds.

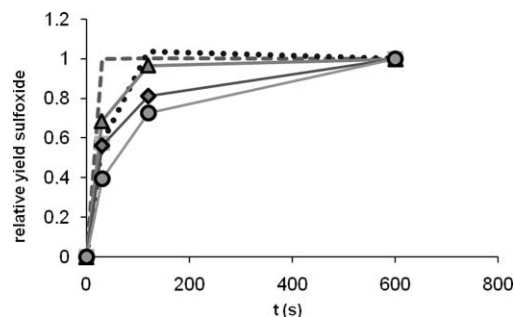


**Fig. 4** Sulfoxidation of thioanisole in time by CPs obtained from filtration of 7 ( $\circ$ ), 23 ( $\diamond$ ) and 36  $\mu\text{M}$  ( $\triangle$ ) dispersions of CPO and PS-PIAT. The data reported are the average of three measurements. The curves obtained with free CPO at 60 nM (dotted line) and 1  $\mu\text{M}$  (dashed line) are also shown.

To study if the same effect was observed for the oxidation of thioanisole as for the oxidation of pyrogallol (Fig. 1), CPs were prepared with the same starting concentrations of CPO, e.g., 7, 23, and 36  $\mu\text{M}$  (Fig. 5) and after 40 s the yields for sulfide oxidation were determined. Within this short reaction time the conversion is still in the linear phase and deactivation of CPO due to hydrogen peroxide is not important.<sup>41</sup> Based on the activity for thioanisole sulfoxidation of the free enzyme the concentration of the enzyme inside the polymersomes was 0.1  $\mu\text{M}$  (enzyme concentration before filtration = 23  $\mu\text{M}$ ), approaching the number calculated for the pyrogallol oxidation. However, with respect to this substrate a trend was now observed in which the initial rate of the reaction,  $V_i$ , was lowest for the polymersomes containing the lowest concentration of enzyme, and  $V_i$  was highest for the polymersomes containing the highest enzyme concentration (see also Fig. 4). Although this is in agreement with the data observed

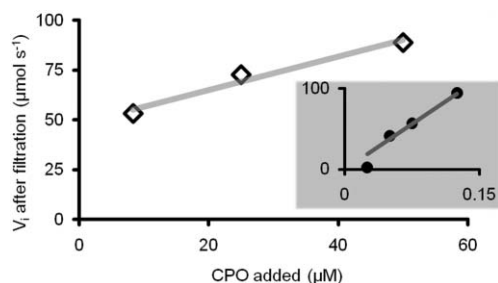


**Fig. 5** Variation of the initial rate of the sulfoxidation of thioanisole of CPs obtained from filtration of 7, 23 and 36  $\mu\text{M}$  dispersions of CPO and PS-PIAT. Upon the increase of enzyme concentration inside the polymersomes, the activity increases as well, as is the case for the free enzyme (inset).

for sulfoxidation by the free CPO, it is in contrast to the results obtained with pyrogallol (compare Fig. 1 and 5).

To explain these observations, we consider that sulfoxidation of thioanisole is a much slower process ( $k_{\text{cat}} = 200 \text{ s}^{-1}$ )<sup>40</sup> than the oxidation of pyrogallol ( $k_{\text{cat}} = 2500 \text{ s}^{-1}$ )<sup>48</sup> and that the kinetics of substrate conversion in the polymersome is a 2-step process (Fig. 6). The first step, represented by the rate constant  $k_{\text{transfer}}$ , involves the diffusion of the substrate molecules into the polymersome, which depends on the membrane properties. The second step is the turnover by the enzyme and is represented by  $k_{\text{cat}}$ , assuming that Michaelis–Menten kinetics is obeyed. The former rate constant,  $k_{\text{transfer}}$ , is a complex parameter and depends on the concentration of the substrate both inside,  $[\text{S}]_{\text{in}}$ , and outside,  $[\text{S}]_{\text{out}}$ , the polymersomes (including such parameters as the local block copolymer structure, the enzyme used, pH and polarity of the solvent). Because of the high  $k_{\text{cat}}$  of pyrogallol by the enzyme, the rate-limiting step for the CPs, in this case, is  $k_{\text{transfer}}$ . For the sulfoxide formation the rate-limiting step is probably turnover by the enzyme, because  $k_{\text{cat}}$  is much lower. In this case  $k_{\text{transfer}} \gg k_{\text{cat}}$  and as a result  $k_{\text{transfer}}$  does not seem to have an effect on the conversion of the thioanisole. The encapsulation of the enzymes into the polymersomes evidently introduces an additional parameter to the enzyme kinetics, that is the ratio  $k_{\text{transfer}}/k_{\text{cat}}$ . At high ratios the substrate conversion by the enzyme is unrestricted while at lower ratios the turnover frequency is dictated by the polymersome properties. This property of the polymersomes is important as it may be useful to tune reaction rates relative to each other in cascade reactions.<sup>31</sup>

The observation that the sulfoxidation activity varied linearly with the enzyme concentration inside the polymersomes suggests that the kinetics can be described by the Michaelis–Menten model. For peroxidases (being two-substrate enzymes) these parameters can be determined when the  $\text{H}_2\text{O}_2$  concentration is kept at saturating concentrations ( $>5 \text{ mM}$ ) and the substrate concentration is varied.<sup>49,50</sup> Determining the kinetic parameters indeed showed that the encapsulated enzyme displayed the same saturation kinetics as the free enzyme and the  $K_{\text{M}}$  for thioanisole appeared to be similar (Table 2 and Fig. S6†). The comparable  $K_{\text{M}}$  suggests that  $[\text{S}]_{\text{in}} = [\text{S}]_{\text{out}}$  and that the kinetics in the case of sulfoxidation with the CPs are determined by step 2 (Fig. 6).

For both the pyrogallol oxidation and the thioanisole oxidation the concentration of CPO inside the polymersomes, determined on the basis of activity, is lower ( $\sim 0.1 \mu\text{M}$ , (enzyme concentration

**Table 2** Kinetic parameters for sulfoxidation of thioanisole by CPs and free CPO

	CP	CPO (20 nM) <sup>a</sup>	CPO (300 nM)
$K_{\text{M}}$	5	4	3
$k_{\text{cat}}$	34 <sup>b</sup>	400	275

<sup>a</sup> Activity determined by UV-Vis. <sup>b</sup> Assuming the enzyme concentration in the polymersomes is that found by direct measurement of the concentration by UV-Vis.

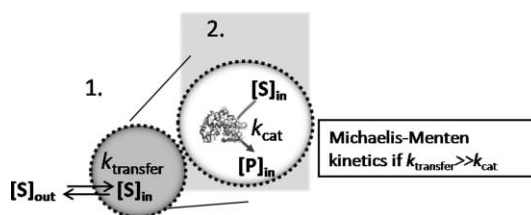


**Fig. 6** Model proposed to explain the different kinetics observed for pyrogallol and thioanisole conversion by chloroperoxidase encapsulated in CPs. Two steps can be discerned: 1) diffusion of the substrate into the polymersome, 2) the conversion of the substrate by the enzyme.

before filtration = 23  $\mu\text{M}$ ) than the concentration measured by optical spectroscopy ( $\sim 0.9 \mu\text{M}$ ). For pyrogallol oxidation this partial deactivation appears to be less relevant, because the rate-limiting step is  $k_{\text{transfer}}$ . For thioanisole oxidation this translates to a value for the turnover number ( $k_{\text{cat}} = 34 \text{ s}^{-1}$ ) that is an order of magnitude lower than the value for the free enzyme ( $k_{\text{cat}} = 400 \text{ s}^{-1}$ ). This lower catalytic efficiency cannot be the result of the  $k_{\text{transfer}}$ , as it was concluded that the diffusion into the membrane is not important for thioanisole.

The decrease in catalytic efficiency could either be caused by a deactivation of the enzyme or by the fact that a significant fraction of the enzyme present in the polymersomes is not accessible to substrate molecules. In the latter case it can be calculated that the activity observed only comes from  $\sim 10\%$  of the encapsulated enzyme molecules. We were able to discriminate between these two possibilities by the observation that 43% of the enzymatic activity could be released from the polymersomes by redispersion of the CPs upon filtration in buffer, while 39% remained in the polymersomes (Fig. S7†). When the activity of the filtrates and the remaining activity in the polymersomes were tested for their protein content similar percentages were found (Fig. S8†), showing that the protein population as a whole was deactivated.

## Conclusion

In this paper we have described the functional encapsulation of chloroperoxidase (CPO) into PS-PIAT polymersomes. It is shown that CPO can be encapsulated with an efficiency of 5% under conditions that favour self-assembly of the PS-PIAT molecules. In the oxidation of pyrogallol catalyzed by CPO, it was found that the activity of the enzyme is 0.4% with respect to the activity before encapsulation. Furthermore, it was observed that there is no linear correlation between the activity of the CPO-containing polymersomes (CPs) and the concentration of the enzyme in the polymersomes, suggesting that the rate of conversion of pyrogallol

is limited by the transfer of substrate molecules over the membrane. In order to show the potential of nano-structured materials for the immobilization of enzymes, we also studied the oxidation of thioanisole to the corresponding (*R*)-sulfoxide, an important organic synthon. Interestingly, this substrate was readily oxidized with the same high enantioselectivity. The kinetic parameters for the oxidation of thioanisole by the CPs suggest that for this reaction the turnover by the enzyme is the rate-limiting factor. The different kinetic behaviours of the substrates is explained by a model that takes into account the rate of diffusion into the polymersomes and the rate of conversion of the substrate by the enzyme.

## Experimental section

UV analysis was performed on a Shimadzu UV-4201 SPC spectrophotometer using an electronic stirrer (Rank Brothers) at 400 rpm at 21 °C. Chiral GC was performed on a Shimadzu GC 17A with AOC-201 automatic injector. Electron microscopy including sample preparation was carried out as reported previously.<sup>30</sup> CFM was carried out with a set-up reported previously.<sup>51</sup> However, to discriminate between fluorescence emission from PS-PIAT ( $\lambda_{em} = 505$  nm) and the fluorescent dye, the enzyme was labelled with Alexa-633 succinimidyl ester and purified following the protocol supplied. The average degree of labelling was 1.4 moles of Alexa-633 per mole of enzyme. Encapsulation was performed under conditions as described in the text.

CPO (EC 1.11.1.10) was bought from BioChemika as a dark-brown suspension in 0.1M phosphate buffer, pH = 4. The suspension was used as received. The stated amount of units was 22731 U ml<sup>-1</sup>. UV showed the  $R_z$  value to be 0.7 (Fig. S9†), and the concentration of the CPO in the solution to be ~25 mg ml<sup>-1</sup> (600  $\mu$ M). Halogenase activity was measured by the monochlorodimedon (2-chloro-5,5-dimethyl-1,3-cyclohexanedione) assay, and peroxidase activity was measured by the pyrogallol (1,2,3-trihydroxybenzene) assay.<sup>38,41</sup> Peroxidase activity was always measured by UV as the increase in absorbance per minute at  $\lambda = 420$  nm. The reaction was initiated by the addition of 50  $\mu$ l of the sample solution to a cuvette containing 2.9 ml of Milli-Q solution (pH = 6), pyrogallol (43 mM) and H<sub>2</sub>O<sub>2</sub> (9 mM). As the assay conditions were constant during the study, pyrogallol activity is reported in AU min<sup>-1</sup>. For thioanisole oxidation typical reaction volumes were 250  $\mu$ l, comprising 100  $\mu$ l of the CPO-containing polymersomes, an additional amount of substrate (always taken from an 18 mM thioanisole stock in milli-Q and extensively dispersed before addition) and an 18 mM solution of H<sub>2</sub>O<sub>2</sub>. The reaction was initiated by addition of the oxidant and shaken on a Thermotwister Comfort (Quantifoil instruments) at 5 rpm at 21 °C. Reaction times were 40 s. After the desired time the reaction was quenched by the addition of Na<sub>2</sub>SO<sub>3</sub>. Complete quenching of the oxidant was checked with peroxide test sticks (Quantofix). The solution was extracted with 0.50 ml DCM containing hexadecane as the internal standard. After drying over a small column of anhydrous magnesium sulfate the phases were separated by spinning down for 10 s and the solution was directly analyzed for yield and ee by GC on a Chiraldex G-TA column (50 m  $\times$  0.25 mm  $\times$  0.12  $\mu$ m), running isothermally at 160 °C for 20 min (column flow: 0.9 ml min<sup>-1</sup>; split ratio: 1/60). Elution times were 7.2 min for (*R*)-methyl phenyl sulfoxide and 11.1 min for (*S*)-methyl phenyl sulfoxide.

## Acknowledgements

Victor I. Claessen (HFML) is acknowledged for help with the CSLM measurements and Dr. M. Koepf for providing the rhodamine-azide. The Research School NRSC-Catalysis, the Royal Netherlands' Academy for Arts and Sciences, and the Chemical Council of the Netherlands Organization for Scientific Research are acknowledged for financial support.

## References

- 1 M. Antonietti and S. Förster, *Adv. Mater.*, 2003, **15**, 1323–1333.
- 2 D. M. Vriezema, M. C. Aragoes, J. A. A. W. Elemans, J. J. L. M. Cornelissen, A. E. Rowan and R. J. M. Nolte, *Chem. Rev.*, 2005, **105**, 1445–1489.
- 3 E. W. Stein, D. V. Volodkin, M. J. McShane and G.B. Sukhorukov, *Biomacromolecules*, 2006, **7**, 710.
- 4 Y. Hu, T. Litwin, A. R. Nagaraja, B. Kwong, J. Katz, N. Watson and D. J. Irvine, *Nano Lett.*, 2007, **7**, 3056.
- 5 J. Kim, J. W. Grate and P. Wang, *Chem. Eng. Sci.*, 2006, **61**, 1017.
- 6 J. Kim, H. F. Jia and P. Wang, *Biotech. Adv.*, 2006, **24**, 296.
- 7 P. Walde and S. Ichikawa, *Biomol. Eng.*, 2001, **18**, 143–177.
- 8 P. Walde and B. Marzetta, *Biotechnol. Bioeng.*, 1998, **57**, 216.
- 9 G. E. Lawson, F. Y. Lee and M.R.A. Singh, *Adv. Funct. Mater.*, 2005, **15**, 267–272.
- 10 H. Burt and K. Letchford, *Eur. J. Pharm., Biopharm.*, 2007, 65.
- 11 Y. Lvov, A. A. Antipov, A. Mamedov, H. Mohwald and G. B. Sukhorukov, *Nano Lett.*, 2001, **1**, 125.
- 12 M. J. Boerakker, N. E. Botterhuis, P. H. H. Bomans, P. M. Frederik, E. M. Meijer, R. J. M. Nolte and N.A. J. M. Sommerdijk, *Chem. Eur. J.*, 2006, **12**, 6071.
- 13 J. Rubio, F. Tamimi Marino and E. Lopez, *J. Biomed. Mater. Res., Part B*, 2007, **83**, 145–152.
- 14 E. A. Simone, T. D. Dziubla, F. Colon-Gonzalez, D. E. Discher and V. R. Muzykantov, *Biomacromolecules*, 2007, **8**, 3914–3921.
- 15 G. Decher, *Science*, 1997, **277**, 1232.
- 16 C. S. Peyratout and L. Dahne, *Angew. Chem., Int. Ed.*, 2004, **43**, 3762–3783.
- 17 A. Yu, Z. Liang and F. Caruso, *Chem. Mater.*, 2005, **17**, 171.
- 18 O. Kreft, M. Prevot, H. Mohwald and G. B. Sukhorukov, *Angew. Chem., Int. Ed.*, 2007, **46**, 5605–5608.
- 19 A. Dyal, K. Loos, M. Noto, S. W. Chang, C. Spagnoli, K. V. Shafi, A. Ulman, M. Cowman and R. A. Gross, *J. Am. Chem. Soc.*, 2003, **125**, 1684.
- 20 K. Kita-Tokarczyk, J. Grumelard, T. Haefele and W. Meier, *Polymer*, 2005, **46**, 3540.
- 21 L. Zhang, K. Yu and A. Eisenberg, *Science*, 1996, **272**, 1777.
- 22 B. M. Discher, Y. Y. Won, D. S. Ege, J. C. M. Lee, F. S. Bates, D. E. Discher and D. A. Hammer, *Science*, 1999, **284**, 1143.
- 23 P. Broz, S. Driamov, J. Ziegler, N. Ben-Haim, S. Marsch, W. Meier and P. Hunziker, *Nano Lett.*, 2006, **6**, 2349.
- 24 H. J. Choi and C. D. Montemagno, *Nano Lett.*, 2005, **5**, 2538.
- 25 J. A. Opsteen, R. P. Brinkhuis, R. L. M. Teeuwen, D.W. P. M. Löwik and J.C.M. van Hest, *Chem. Commun.*, 2007, 3136.
- 26 B. Li, A. L. Martin and E. R. Gillies, *Chem. Commun.*, 2007, 5217.
- 27 S. F. M. Van Dongen, M. Nallani, S. Schoffelen, J. J. L. M. Cornelissen, R. J. M. Nolte and J.C.M. van Hest, *Macromol. Rapid Commun.*, 2008, **29**, 321.
- 28 M. Nallani, S. Benito, O. Onaca, A. Graff, M. Lindemann, M. Winterhalter, W. Meier and U. Schwaneberg, *J. Biotechnol.*, 2006, **123**, 50–59.
- 29 D. M. Vriezema, J. Hoogboom, K. Velonia, K. Takazawa, P. C. M. Christianen, J. C. Maan, A. E. Rowan and R. J. M. Nolte, *Angew. Chem., Int. Ed.*, 2003, **42**, 772.
- 30 H.-P. M. de Hoog, D. M. Vriezema, M. Nallani, S. Kuiper, J. J. L. M. Cornelissen, A. E. Rowan and R. J. M. Nolte, *Soft Matter*, 2008, **4**, 1003–1010.
- 31 D. M. Vriezema, P. M. L. Garcia, N. S. Oltra, N. S. Hatzakis, S. M. Kuiper, R. J. M. Nolte, A. E. Rowan and J. C. M. van Hest, *Angew. Chem., Int. Ed.*, 2007, **46**, 7378.
- 32 R. A. Sheldon, I. W. C. E. Arends and U. Hanefeld, *Green Chemistry and Catalysis*, Wiley-VCH, 2007.

- 
- 33 A. Kawamura, A. Harada, K. Kono and K. Kataoka, *Bioconjugate Chem.*, 2007, **18**, 1555.
- 34 N. Bruns and J. C. Tiller, *Nano Lett.*, 2005, **5**, 45.
- 35 V. M. Dembitsky, *Tetrahedron*, 2003, **59**, 4701–4720.
- 36 C. E. Grey, M. Hedström and P. Adlercreutz, *ChemBioChem*, 2007, **8**, 1055–1062.
- 37 M. Nallani, H.-P. M. de Hoog, J. J. L. M. Cornelissen, A. R. A. Palmans, J. C. M. van Hest and R. J. M. Nolte, *Biomacromolecules*, 2007, **8**, 3723–3728.
- 38 D. R. Morris and L. P. Hager, *J. Biol. Chem.*, 1966, **241**, 1763.
- 39 J. A. Thomas, D. R. Morris and L. P. Hager, *J. Biol. Chem.*, 1970, **245**, 3129.
- 40 F. Van Rantwijk and R. A. Sheldon, *Curr. Opin. Biotechnol.*, 2000, **11**, 554–564.
- 41 J. B. Park and D. S. Clark, *Biotechnol. Bioeng.*, 2006, **93**, 1190–1195.
- 42 P. F. Hallenberg and L. P. Hager, *Methods Enzymol.*, 1978, **52**, 521–529.
- 43 J. Gawronski, J. Grajewski, J. Drabowicz and M. Mikolajczyk, *J. Org. Chem.*, 2003, **68**, 9821–9822.
- 44 S. Kobayashi, M. Nakano and T. Goto, *Biochem. Biophys. Res. Commun.*, 1986, **135**, 166–171.
- 45 S. Colonna, N. Gaggero, A. Manfredi, L. Casella, M. Gullotti, G. Carrea and P. Pasta, *Biochemistry*, 1990, **29**, 10465–10468.
- 46 S. Lutz, K. Vuorilehto and A. Liese, *Biotechnol. Bioeng.*, 2007, **98**, 525–534.
- 47 N. Spreti, R. Germani, A. Incani and G. Savelli, *Biotechnol. Prog.*, 2004, **20**, 96–101.
- 48 M. B. McCarthy and R. E. White, *J. Biol. Chem.*, 1983, **258**, 9153–9158.
- 49 R. B. Bhatia, C. J. Brinker, A. K. Gupta and A. K. Singh, *Chem. Mater.*, 2000, **12**, 2434–2441.
- 50 P. Toti, A. Petri, V. Pelaia, A. M. Osman, M. Paolini and C. Bauer, *Biophys. Chem.*, 2005, **114**, 245–251.
- 51 M. Comellas-Aragonès, H. Engelkamp, V. I. Claessen, N. A. J. M. Sommerdijk, A. E. Rowan, P. C. M. Christianen, J. C. Maan, B. J. M. Verduin, J. J. L. M. Cornelissen and R. J. M. Nolte, *Nat. Nanotechnol.*, 2007, **2**, 635.